Bulletin of Earthquake Engineering (2021) 19:2919–2940
https://doi.org/10.1007/s10518-021-01097-x

ORIGINAL ARTICLE

The influence of the frequency content of ground motion on the nonlinear dynamic response and seismic vulnerability of historical masonry towers

Mohammad Amir Najafgholipour[1] · Hossein Darvishi[2] · Mahmoud Reza Maheri[3]

Received: 14 August 2020 / Accepted: 7 April 2021 / Published online: 15 April 2021

Abstract
Observations made on the response of historical masonry towers during past earthquakes indicate that in addition to the intensity of the ground shaking, the frequency content of shaking also affects the seismic performance of these monuments. To evaluate this phenomenon, the influence of the mean period of the ground motion (T_m), as a frequency content indicator, on the seismic behavior of the towers is assessed. To this end, first, the vulnerability of four towers with different aspect ratios and vibration periods (T_s) are evaluated by means of the Incremental Dynamic Analysis (IDA). For this purpose, 37 ground motion records, corresponding to the stations located in sites with different types of soil, are utilized. The nonlinear time history analyzes of the towers are carried out using the OPENSEES software by means of an Equivalent Beam Element with fiber sections. In order to investigate the effects of the frequency content of the ground motion on the seismic response of the towers, for every tower, the variation of the PGA of the ground motion and the induced internal force in the tower at the point of failure are plotted against the period ratio (T_m/T_s). According to the analysis results, it is found that the failure PGA increases as the period ratio becomes smaller. It is also noted that the induced shear in the tower exhibits a similar trend.

Keywords Seismic vulnerability · Historical tower · Masonry · Incremental dynamic analysis · Mean period of the ground motion

✉ Mohammad Amir Najafgholipour
najafgholipour@sutech.ac.ir

[1] Faculty of Civil and Environmental Engineering, Shiraz University of Technology, Shiraz, Iran

[2] Graduate Student of Civil and Environmental Engineering, Shiraz University of Technology, Shiraz, Iran

[3] Department of Civil and Environmental Engineering, Shiraz University, Shiraz, Iran

1 Introduction

Slender masonry structures, such as fortress towers, clock towers, the bell towers of churches, the minarets of mosques, etc. are found throughout the world. Many of these structures are historical monuments of great cultural value. A majority of these monuments have not been designed to withstand seismic loads. In addition, deterioration of their materials and components over time under adverse environmental conditions may have resulted in development of cracks and weakened their load bearing elements.

In order to determine the dynamic characteristics of existing masonry towers and to investigate their performance under different types of loading, especially the ground motion excitation in an earthquake, extensive case studies have been conducted on real historical towers (D'Ambrisi et al. 2012; Saisi et al. 2015; Bartoli et al. 2017a, b; García-Macías and Ubertini 2019; Invernizzi et al. 2019; Micelli and Cascardi 2020). In this regard, usually a combination of material tests (less destructive or non-destructive), in situ non-destructive structural tests such as ambient vibration test, and Finite Element (FE) analysis are carried out. Accordingly, structural characteristics of the towers; including the material properties of different parts of the towers, the real boundary conditions and dynamic characteristics of the towers, including the natural vibration frequencies and the corresponding mode shapes are identified. In a number of studies, nonlinear time history analysis of towers have been carried out through detailed FE models to obtain an insight about the seismic performance of the towers. Some studies have also been conducted on the health monitoring of existing masonry towers (Anzani et al. 2010; Cavalagli et al. 2017); other studies have assessed damage to these monuments during earthquakes (Saisi et al. 2015). In a report, Romaro (2011), presented the failure modes of some historical towers in past earthquakes. Shaking table test along with nonlinear FE analysis were carried out to evaluate the seismic performance of typical historical towers in China (Xie et al. 2020).

Numerical studies have been conducted to assess the seismic vulnerability of existing masonry towers (Casolo et al. 2013; Preciado 2015; Castellazzi et al. 2018; Torelli et al. 2020). Valente and Milani (2016b) investigated the seismic performance of some historical towers in Italy through nonlinear time history analysis using the FE software ABAQUS. Simplified simulation techniques have also been proposed for the time history analysis of slender masonry structures. For instance, Peña et al. (2010) used a three-dimensional beam model for the simulation of the Qutb Minar Tower in India. The flexibility of the soil beneath the foundation and the soil-structure interaction, which can significantly affect the dynamic response of the towers as well as the distribution of damage along their heights, were simulated in a number of numerical studies (Casolo et al. 2017; de Silva et al. 2018; Silva 2020).

In order to evaluate the seismic vulnerability of masonry towers, different methodologies have been used (Valente and Milani 2016a, b; Facchini et al. 2017; Sarhosis et al. 2018). For instance, in a number of studies, the nonlinear static analysis method was utilized to evaluate the seismic performance of the towers (Pintucchi and Zani 2014; Bocciarelli and Barbieri 2017) Recently, Incremental Dynamic Analysis (IDA) method has been used for the vulnerability assessment of existing structures. This analysis technique was used by Marra et al. (2017) to assess the seismic performance of historical masonry towers. A simplified rigid block and spring model was used to simulate the towers in the IDA procedure.

Due to the special shape of historical towers, their dynamic characteristics, particularly their fundamental vibration frequency, play crucial roles in their performance under

dynamic loads such as wind or earthquakes. Several empirical, semi-analytical and analytical formulations have been developed to estimate the fundamental vibration frequency of towers (Shakya et al. 2016; Bartoli et al. 2017a, b; Diaferio et al. 2018; Najafgholipour et al. 2019). Some of these relations have been employed in codes and standards for practical response evaluation and design.

Observations made after numerous past earthquakes, show that these slender structures have a somewhat different and unexpected behavior compared to other structures. For instance, it has been noted that in regions where low-rise buildings suffered extensive damage, the slender masonry towers experienced minor damage. Conversely, in some low or moderate intensity earthquakes, while other buildings experienced only minor damage, the towers suffered more and some collapsed. The former case was observed in 2016 Italy earthquake in which the clock tower of Amatrice was still standing with relatively minor damage, whereas, the surrounding buildings suffered extensive damage (see Fig. 1). Maheri (2004) also investigated the behavior of masonry towers in Iran during past earthquakes and reached similar conclusions.

This, somewhat unique, performance of masonry towers during earthquakes confirms that in addition to the magnitude of the earthquake, the characteristics of ground motion including its frequency content and duration, affect dynamic response of these monuments. In other words, a tower with specific material and geometrical properties may exhibit different performances (may collapse or remain undamaged) under different ground shakings with a similar intensity. However, in a common design or performance assessment of these structures, this phenomenon cannot be identified in static or regular dynamic analysis of the structures.

The influence of the frequency content of ground motion on the dynamic response of structures and building frames has been investigated in a number of studies (Kumar et al. 2011; Hickey and Broderick 2019). However, only a limited number of studies have addressed this issue for masonry towers (Casolo et al. 2017). In this study, the effects of the frequency content of ground motions on the nonlinear time history response of masonry towers have been investigated. For this purpose, four towers with different fundamental vibration periods (T_s), which were primarily designed to withstand wind load, are analyzed using 37 ground shaking records. The ground motions belong to the stations located in sites with two types of soil. The mean periods (T_m) of the records, as the common frequency content indicator for ground motions, are determined. In order to find the induced

Fig. 1 The Amartice bell tower was still standing after 2016 Italy earthquake

Table 1 Geometrical details of the selected towers

Tower	Height H (m)	Section width L (m)	Wall thickness t (m)
Tower 1	20	6.25	1.5
Tower 2	30	7.00	1.5
Tower 3	40	7.75	1.5
Tower 4	50	8.50	1.5

Table 2 Material properties of the selected towers

Mechanical property	Value
Elastic modulus (MPa)	800
Compressive strength (MPa)	2.41
Tensile strength (MPa)	0.04
Mass density (kg/m^3)	2000

base shear in the towers and the peak ground acceleration (PGA) corresponding to the failure of the towers, Incremental Dynamic Analysis (IDA) is utilized. Finally, the influence of the ratio of the mean period of the ground motions to the fundamental period of vibration of the towers (T_m/T_s) on the PGA of ground motion and the induced shear in the tower at the stage of failure are evaluated. In this way, the effects of two major influential variables, including the frequency content and PGA of ground motion are evaluated simultaneously. In addition, the dominant parameter in the performance of towers is found.

2 The selected towers

Four prismatic towers with square box sections and identical material properties were considered for numerical investigation. The cross sectional dimensions of the towers were selected to range between 6.25 and 8.5 m. However, a constant thickness of 1.5 m was considered for the walls of all towers. The towers had different heights, leading to different aspect ratios with vibration periods. The geometrical properties of the towers are listed in Table 1. It should be noted that the towers were primarily designed for wind loads, based on the Iranian Building Code (2013). The assumed properties for the masonry material, including the mass density, tensile strength, compressive strength and elastic modulus were adopted from a case study reported previously by Valente and Milani (2016a, b) (see Table 2). The stress–strain curves of the masonry in tension and compression are also illustrated in Fig. 2.

3 Modeling the towers

Detailed numerical modeling and seismic analysis of historical masonry towers, by using their actual geometry and material properties require a relatively high computational effort. Therefore, alternative modeling strategies, in which the global behavior of the towers takes prime position, are preferred to save time and computational cost. As a brief review on the seismic analysis of the masonry towers, it can be stated that in some studies the simplified

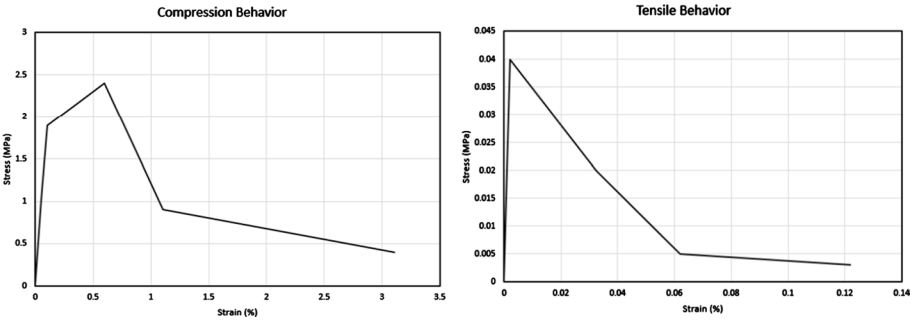

Fig. 2 The stress–strain curves of masonry in tension and compression (Valente and Milani 2016a, b)

'discrete element model' is used for simulation of masonry towers (Marra et al. 2017). This model, which is also called; the 'rigid body and spring model', consists of rigid blocks and nonlinear springs for simulating the nonlinear behavior of masonry material. Other methods; such as the 'three-dimensional beam model' and 'in-plane rigid model' (rigid elements and springs) were also used by Peña et al. (2010) to simulate nonlinear dynamic behavior of the Qutb Minar tower.

In order to perform a large number of nonlinear time history analyzes using the IDA procedure, a reasonably accurate, yet simple model is required. For this purpose, in the present paper, by considering the three-dimensional beam model proposed by Peña et al. (2010), an equivalent beam element with fiber section, already implemented in OPENSEES software, is utilized. The details of the model and its numerical validation are described in the following sections.

3.1 Introducing the equivalent beam element with fiber section

The fiber beam model is a reliable element which consists of a number of finite fibers in each cross section. This model is based on the assumption of linear geometry, which is accepted and widely used due to its simplicity and accuracy in modeling nonlinear behavior of structural elements. By this assumption, the cross sections are not distorted and plane sections remain plane and normal to the longitudinal axis. In this model, only the uniaxial constitutive behavior of the material along the axis of the element is required.

In the present paper, to model masonry towers, the fiber beam model was utilized; see Fig. 3. In this way, the towers with variable cross sections along their heights, as well, as those with layered walls, can be simulated. Due to more or less flexural behavior of slender masonry towers, having a large height (H) to depth (L) ratio, where the shear deformations are negligible, using this simplified model is reasonable.

3.2 Validation of the equivalent beam element for simulation of masonry towers

In cantilever structural elements, such as structural walls having aspect ratios greater than 2.0, it is reported that, in both the elastic and inelastic ranges, flexural behavior is dominant (Najafgholipour et al. 2014; Maheri et al. 2019). The aspect ratios of towers investigated in this study are greater than 3.0. Therefore, the towers are expected to respond primarily in flexure, hence using the simple equivalent beam element, which does not consider

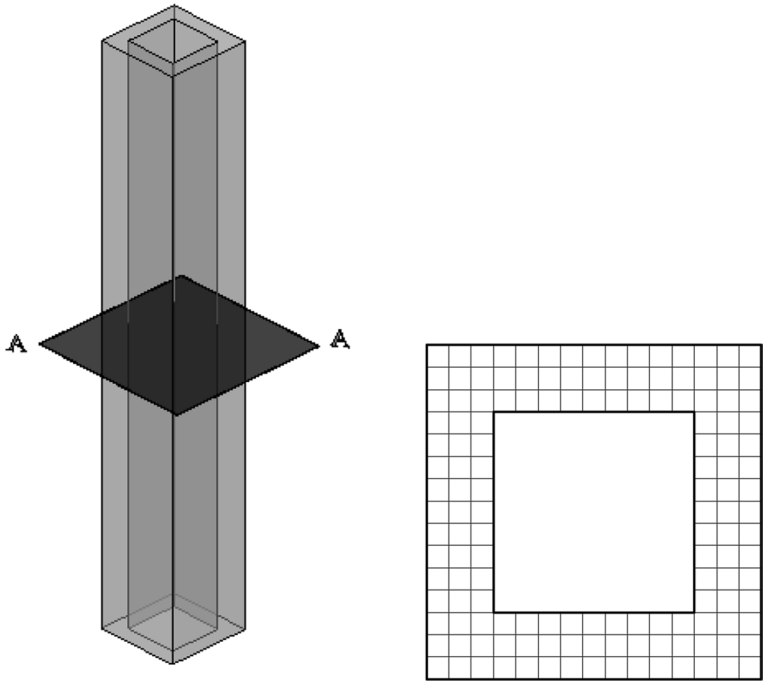

Fig. 3 Modeling the masonry towers using the Equivalent Beam Element with fiber section

shear deformations, is justified. To verify this point and the validity of the equivalent beam element in modeling the seismic behavior of masonry towers with an acceptable level of accuracy, two sets of validation were conducted, including: (1) evaluating the fundamental periods of the set of four towers listed in Table 1 and (2) evaluating the main natural frequencies and the nonlinear pushover response of the Qutb Minar in India.

3.2.1 Fundamental periods of vibration

The vibration periods of the towers listed in Table 1, were determined using three different methods of: (1) the equivalent beam element with fiber sections presented in Sect. 3.1, (2) the empirical formulation proposed by Bartoli et al. (2017a, b) and (3) the numerical simulation of towers with 3D solid elements in the ABAQUS finite element software. The results of these free vibration analyses on towers are compared in Table 3.

Table 3 Fundamental periods of vibration of the selected towers

Tower	Equivalent beam element	Bartoli et al. (2017a, b)	3D FE simulation
Tower 1	0.56	0.65	0.6
Tower 2	1.10	1.25	1.14
Tower 3	1.72	1.96	1.76
Tower 4	2.44	2.74	2.42

Table 3 shows that the differences between the fundamental periods of vibration of the towers determined using the 3D FE simulation and the idealized equivalent beam model are between 1 and 7%, which are not considerable for masonry towers. Since the masses of the structures in both models are the same, the differences in periods are related to the stiffness of the towers. It should be noted that, since an equivalent beam model is somewhat stiffer in flexure compared to the 3D FE model, the differences in towers' stiffness when using the FE simulation and the idealized equivalent beam model are only partially due to the effects of shear deformations. Consequently, although shear deformations are not considered in the idealized equivalent beam models, this omission does not appear to significantly affect the dynamic characteristics of towers. Furthermore, some of the towers were analyzed under a number of ground shakings with a range of mean periods. The analyses results indicated that the dominant mode of failure in these models were indeed flexural. On the other hand, the differences between results of the empirical formulation proposed by Bartoli et al. (2017a, b) and those obtained from the two numerical studies are noticeable (see Table 3).

3.2.2 Qutb Minar tower

The Qutb Minar tower is about 70 m high and has a complex texture and a relatively complex geometry. The circular cross section of the tower is composed of several layers with different material properties varying along the height of the structure. A vertical section of this tower is illustrated in Fig. 4. This monument has been the subject of experimental and numerical studies conducted by Peña et al. (2010), in which its material properties and dynamic characteristics were determined. They used not only a 3D, FE model to analyze

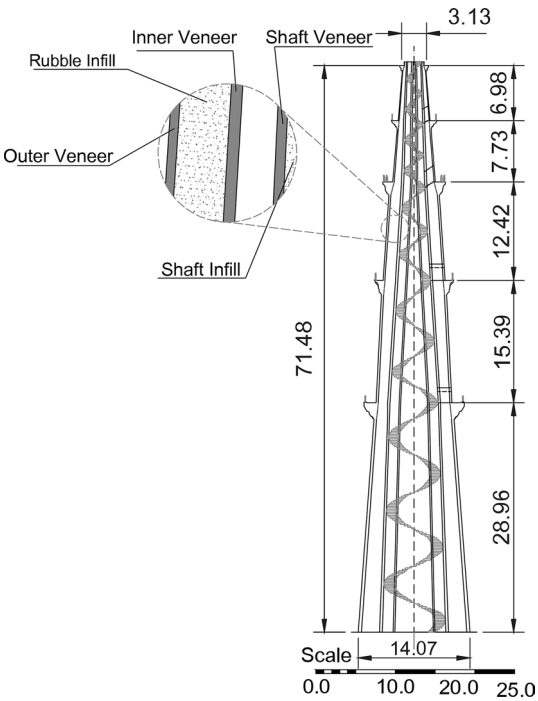

Fig. 4 The geometrical details of the Qutb Minar Tower (Peña et al. 2010)

Table 4 Material properties of the Qutb Minar Tower (Mendes 2006)

	Density (kg/m^3)	Modulus of elasticity (GPa)	Poisson ratio	Comressive strength (MPa)	Tensile strength (MPa)
Shaft infill 1–3	1800	2.0	0.2	2.0	0.05
Shaft infill 4–5	1800	0.6	0.2	0.6	0.05
Shaft veneer	2600	5.21	0.2	5.2	0.05
Stairs	2000	3.69	0.2	–	–
Inner veneer Layer 1–3	2600	5.21	0.2	5.2	0.05
Inner veneer Layer 4–5	2300	2.5	0.2	2.5	0.05
Rubble Infill Layer 1–3	1800	2.0	0.2	2.0	0.05
Rubble infill Layer 4–5	1800	0.6	0.2	0.6	0.05
Outer veneer Layer 1–3	2300	2.5	0.2	2.5	0.05
Outer veneer Layer 4–5	2600	3.0	0.2	3.0	0.05

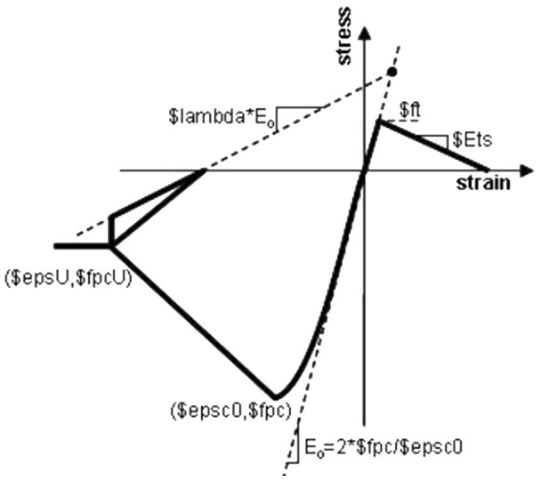

Fig. 5 The Concrete02 material model in OPENSEES

this monument, but also examined other simplified models such as the three-dimensional beam model for nonlinear analysis of the tower. The material properties of different parts of the tower, in height and thickness, are listed in Table 4.

As it was stated, in this study simulation of the towers, including the Qutb Minar, was carried out by means of the Equivalent Beam Element with fiber section in OpenSEES software. To define the uniaxial stress–strain behavior of the masonry material in tension and compression, as an appropriate model for brittle and semi-brittle materials, the Concrete02 constitutive model from the OpenSEES material library was selected; see Fig. 5. The beam model used for simulating the Qutb Minar was in accordance with the geometrical and material specifications which had been determined by Pena et al. (2010). It should be noted that all the towers were assumed to be fixed base in this study.

Two types of analyzes were conducted on the tower. First, through a frequency analysis, the vibration frequencies of the structure were determined by means of the equivalent beam element. The results obtained from the idealized model and those determined

Table 5 The vibration frequencies of the Qutb Minar (Hz)

Mode number	Equivalent beam element (this study)	Experimental results (Peña et al. 2010)	Three dimensional beam model (Peña et al. 2010)
1	0.70	0.79	0.73
2	2.25	1.96	2.26
3	4.47	3.85	4.13

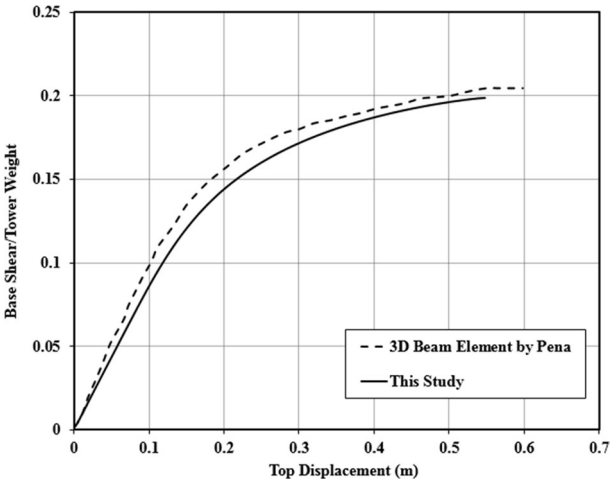

Fig. 6 The nonlinear load–displacement curves of the Qutb Minar tower

from the ambient vibration test, as well as the three-dimensional beam model by Peña et al. (2010) are compared in Table 5. Due to symmetry of the structure, each mode number in the Table 5 stands for a couple of lateral vibration modes along two orthogonal directions. It can be seen that differences in results obtained from the idealized model and those reported by Peña et al. (2010), especially in lower frequencies, are small; therefore it can be concluded that the equivalent beam element can simulate the dynamic behavior of the tower with reasonable accuracy.

Second, the equivalent beam element was also utilized to conduct a nonlinear pushover analysis on the Qutb Minar. For this purpose, it was assumed that the lateral load distribution along the height of the tower is uniform. Comparison of the nonlinear load–displacement curves obtained from this study and that reported by Peña et al. (2010), analyzed using the three-dimensional beam model (see Fig. 6), confirms the ability of the idealized beam model in OPENSEES in modeling the nonlinear behavior of the tower.

4 Incremental dynamic analysis (IDA) of the masonry towers

Many researchers have dedicated a great deal of time and effort to develop procedures for assessing the seismic performance of different types of structures. In this regard, a variety of analysis methods and analytical models have been proposed. Although nonlinear static analysis is widely used in different studies and even for practical assessment projects,

it does not consider the dynamic response of the structures to ground motion directly. The nonlinear dynamic analysis has been utilized for a realistic performance assessment of structures affected by seismic loads. In traditional dynamic analysis, the response of a structure is evaluated under a limited number of ground motions, while it is probable that the performance of a structure depends on the selected ground motion.

On this basis, the Incremental Dynamic Analysis (IDA) was introduced (Vamvatsikos and Cornell 2002). The IDA is a method of analysis in which the structure is subjected to one or more ground motion records, each with several intensity levels. The results of IDA for a specific structure are presented with a graph. Accordingly, the vertical axis of the graph is the intensity level, such as Peak Ground Acceleration (PGA) or Spectral Acceleration and its horizontal axis denotes the response of the structure, such as Maximum Roof Displacement. Different criteria are defined in literature as the failure point of IDA curves. For instance, in FEMA 350 (2000), the last point on each curve with a slope equal to 20% of the elastic slope (initial slope) is defined as the capacity point. This approach is utilized in this study to define the failure point of the IDA curves.

4.1 Selection of the ground motion records

The frequency content of the ground motion records measured in different sites depends on a number of parameters, including; the seismic source characteristics, the distance of the seismic source to the site and the soil type, as well as its profile in depth. Therefore, it is important to have information about the soil characteristics in a station that the ground motion is recorded. Different codes for seismic design of structures classify the soils according to the shear wave velocity within a specific depth of the soil profile. For instance, in ASCE 7-16 the site soil is classified in six categories based on the shear wave velocity in the 30 m depth of the soil profile (V_{s30}) (see Table 6). The higher the shear wave velocity, the stiffer the soil.

In this study, to investigate the dynamic response of masonry towers subjected to ground motion records with a wide range of frequency contents, 37 ground accelerations, measured in the stations on both stiff and soft soils, were selected from the Pacific Earthquake Engineering Research (PEER) database. Details of the selected acceleration records, which correspond to the sites with V_{s30} more than 760 m/s (Rock and Hard Rock) and less than 180 m/s (Soft Soil), are listed in Tables 7 and 8, respectively.

In order to perform an IDA on masonry towers, first, the ground motion records, having a variety of PGAs, were normalized to the PGA of 1.0 g. The response spectrum of the normalized ground motions are plotted in Fig. 7. Then, the intensity (PGA) of each record was divided into equal steps of 0.05 g. Therefore, the initial PGA of each record was 0.05 g and it was increased with an incremental rate of 0.05 g in every step until it reached the

Table 6 Classification of soil according to ASCE 7–16 (2016)

Site class	V_{S30}
A. Hard rock	> 1500 m/s
B. Rock	760 to 1500 m/s
C. Very dense soil and soft rock	360 to 760 m/s
D. Stiff soil	180 to 360 m/s
E. Soft clay soil	< 180 m/s

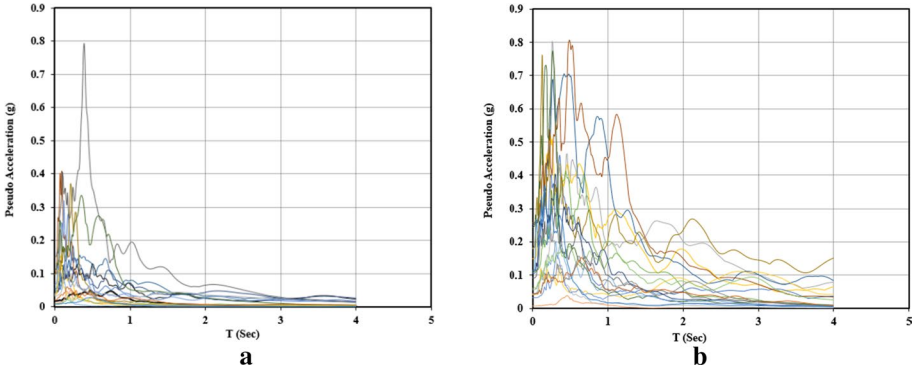

Fig. 7 The response spectrum of the ground motions. **a** Rock soil, **b** soft soil

final intensity (PGA) corresponding to the failure of the tower. Finally, a series of nonlinear dynamic analyses were performed using each ground motion with different PGAs and the maximum lateral displacement at the top of the tower, corresponding to each time history analysis, was determined.

4.2 Simulation and analysis of the towers

The masonry towers introduced in Sect. 2 were also simulated using the Equivalent Beam Element with fiber section in OPENSEES software. Similar to that described in the verification section, the Concrete02 material model was utilized for modeling the stress–strain behavior of masonry fibers in tension and compression. The values of the material properties were adopted from those reported in a numerical study by Valente and Milani (2016a, b) on eight historical towers in Italy (see Table 2).

4.3 The results

Results of the IDA on four towers with different aspect ratios subjected to different earthquake records are presented in Fig. 8. In diagrams of Fig. 8, the vertical and horizontal axes are the PGA of the ground motion and the normalized maximum lateral displacement at the top of the tower (maximum top displacement/height of the tower (δ/H)), respectively. The first point to note from the IDA results of Fig. 8 is that the response of towers to different ground accelerations shows a wide dispersion. This scattering not only exists in the intensity of the ground motion causing the failure of the towers (failure PGA), but also it is evident in the slope of the curves. For instance, in the case of 20 m high tower, the PGAs of the earthquake records causing failure of the tower range from 0.23 g to more than 1.2 g. For the 50 m high tower, the range is even wider; from 0.07 g to around 3.0 g. This means that, for example, the 50 m high tower may be destroyed in a certain 'weak' earthquake with a PGA = 0.07, but it can survive other 'very severe' earthquake with PGAs higher than 1.0 g.

In order to better visualize the distribution of failure PGAs, the results are presented by means of histograms as plotted in Fig. 9. It can be seen that the majority of earthquakes causing failure of these towers have PGAs in the range of 0.2 g to 0.6 g. However, in a number of cases, the towers can survive severe earthquakes with higher PGAs. Moreover,

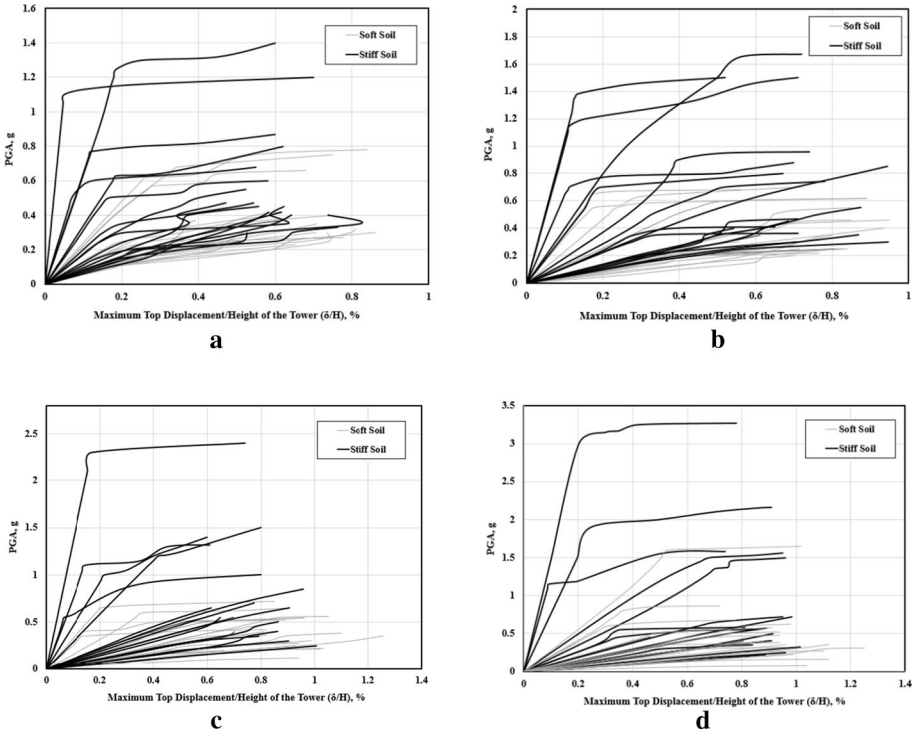

Fig. 8 The Incremental Dynamic Analysis diagrams of the investigated masonry towers with height of **a** 20 m, **b** 30 m, **c** 40 m and **d** 50 m

in some cases the towers collapsed in a slight ground shaking. For instance, the failure PGA of 0.35 g is the most common for the 50 m high tower. However, as it was stated, this tower fails under a particular ground motion with PGA of 0.07 g, but under ground shakings having other frequency contents it could survive much more severe earthquakes with PGA of more than 1.0 g. This phenomenon may justify the survival of some historical towers in past destructive earthquakes.

The mean failure PGA (average of all earthquake records) of the 20 m, 30 m, 40 m and 50 m tall towers are evaluated as 0.45 g, 0.51 g, 0.54 g and 0.63 g, respectively. These values indicate that the mean failure PGA increases as the tower becomes more slender with higher vibration period.

In contrast to the framed buildings, in the slender masonry towers, there are usually little irregularities in plan and elevation and they do not have a high degree of redundancy. Therefore, it is expected that these towers to primarily act as a Single Degree of Freedom (SDOF) system. Therefore, the fundamental mode of vibration and the corresponding period control the seismic behavior of these monuments.

Based on the above discussion related to the dynamic behavior of towers and structural characteristics of these structures, it is inferred that in addition to the intensity of the ground shaking, other factors such as the frequency content of the ground motion may affect the seismic performance of the towers. Further discussions regarding this phenomenon are provided in the subsequent sections.

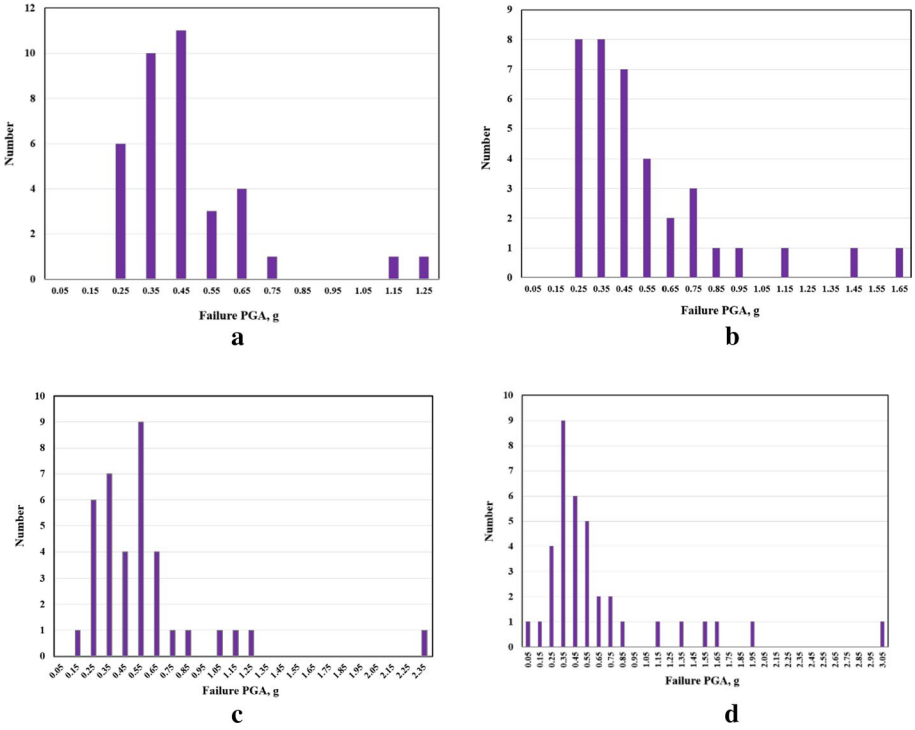

Fig. 9 The histograms of the failure PGAs of towers with height of **a** 20 m, **b** 30 m, **c** 40 m and **d** 50 m

5 The effect of ground motion frequency content on the seismic performance of towers

There are several indicators and parameters introduced in literature to demonstrate the frequency content of a ground motion, such as the predominant period (T_P), the mean period (T_m), spectral velocity-acceleration ratio period ($T_{V/A}$), and the smoothed spectral predominant period (T_0). Among these, the mean period is known as the parameter that shows the frequency content of the ground motions well (Rathje et al. 2004). The mean period of the ground motion is the weighted mean of the periods of the Fourier Amplitude Spectrum (FAS) of a ground motion in a specified frequency range (0.25 Hz to 20 Hz). In contrast to the other frequency content indicators, the mean period is calculated using the FAS, which makes it prominent in characterizing the frequency content of a ground motion. The mean period is calculated as follows:

$$T_m = \frac{\sum_i FA_i^2(1/f_i)}{\sum_i FA_i^2} \quad \text{For } 0.25\,\text{Hz} \le \text{fi} \le 20\,\text{Hz}, \Delta f \le 0.05\,\text{Hz} \tag{1}$$

where FA_i is the Fourier amplitude, f_i is the frequency corresponding to the FA_i and Δf is the frequency interval.

The mean period of the ground motions utilized in this study are listed in Tables 9 and 10. As it can be seen, the selected ground motions cover a range of mean period 0.12 s to 1.94 s.

Another parameter which represents the frequency content of a ground shaking record is the spectral velocity-acceleration ratio period ($T_{V/A}$) (Lee 2009). This parameter depends on the magnitude, distance from the fault, peak ground acceleration (PGA) and peak ground velocity (PGV), and is defined as follows:

$$T_{V/A} = 2\pi.\frac{PGV}{PGA}.\frac{\alpha_V}{\alpha_A} \tag{2}$$

where α_V and α_A are the amplification factors, derived from statistical studies and are related to the magnitude and distance from the fault.

In this study, the mean period (T_m) of the ground motion was utilized to characterize its frequency content. On the other hand, the fundamental vibration period of the towers (T_s) has also a significant role in the dynamic response of these structures. Therefore, the influence of these two parameters are combined as a ratio; the ratio of the mean period of the ground motion (T_m) to the fundamental period of vibration of the tower (T_s), and the effects of this ratio on the nonlinear dynamic response of the towers is evaluated. It should be noted that the period ratio (T_m/T_s) is equivalent to the frequency ratio ($\beta = \omega_f/\omega$) in structural dynamics.

5.1 The effect of period ratio (T_m/T_s) on the failure PGA

In this section, the influence of the period ratio (T_m/T_s) on the failure PGA is investigated. For this purpose, the variation in the failure PGA with changing period ratio (T_m/T_s) is plotted in Fig. 10.

It can be noted that, for all the investigated towers the change in failure PGA with changing period ratio (T_m/T_s) has almost a similar trend. Accordingly, the towers can survive a more severe ground shaking with higher PGA when the mean period of the ground motion is considerably less than the vibration period of the structure. According to the curves, when the period ratio (T_m/T_s) is more than a specific value, this ratio has a slight influence on the failure PGA and results only exhibit some dispersion. For instance, in the tower with height of 20 m, the period ratio more than 1.0 does not affect the failure PGA significantly. This limit is around 0.5, 0.35 and 0.25 for towers with heights of 30 m, 40 m and 50 m, respectively.

To better visualize the effects of the period ratio (T_m/T_s) on the failure PGA of the towers, the results corresponding to all towers are plotted on a diagram in Fig. 11. This diagram confirms that the failure PGA of the towers increases drastically by reducing the period ratio (T_m/T_s). This influence is more significant when the period ratio (T_m/T_s) is less than 0.1. Although the period ratios more than 0.5 do not affect the failure PGA significantly, a slight increase of the failure PGA can be observed for period ratios more than 1.0. This trend confirms the response magnification of the tower when the period ratio approaches 1.0.

In addition, to highlight the fact that the mean period represents the frequency content of ground motion, the failure PGA of towers have been plotted against the period ratio, which is calculated using the spectral velocity-acceleration ratio period ($T_{V/A}$) (see Fig. 12). Accordingly, the variation of failure PGA with T_m/T_s and $T_{V/A}/T_s$ exhibit an almost similar trend.

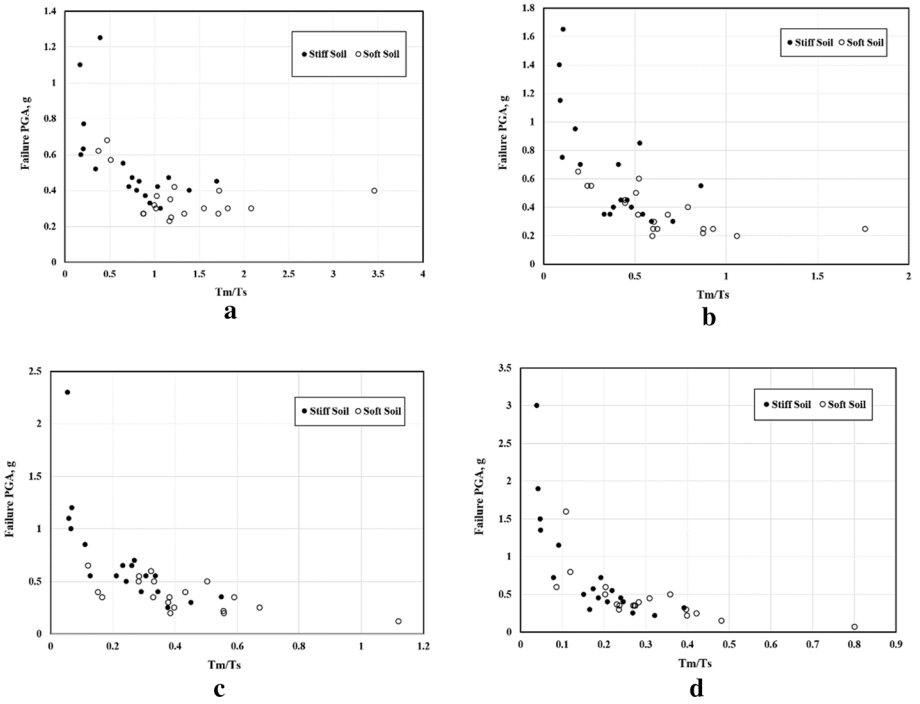

Fig. 10 Variation of the failure PGA with period ratio (T_m/T_s) for towers with height of **a** 20 m, **b** 30 m, **c** 40 m and **d** 50 m

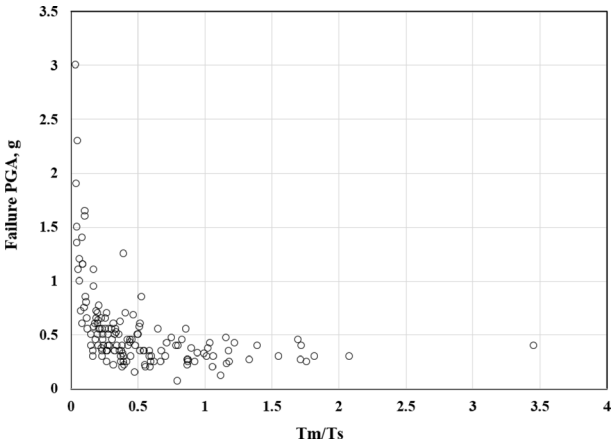

Fig. 11 Variation of the failure PGA with period ratio (T_m/T_s) for all data

5.2 The effect of period ratio (T_m/T_s) on the failure base shear

In order to investigate the effect of the period ratio on the induced shear force in towers at the point of failure, the variations of the failure base shear (V_{bf}) with changing period ratio (T_m/T_s) for different towers are plotted in Fig. 13.

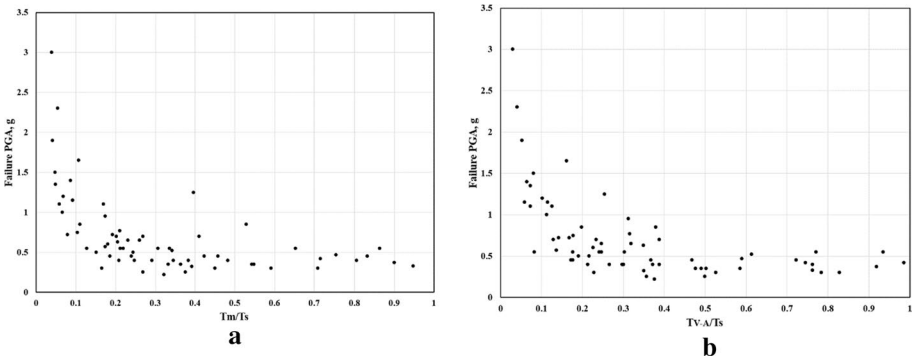

Fig. 12 Variation of the failure PGA related to records measured on rock with period ratio using **a** Tm, **b** $T_{V/A}$

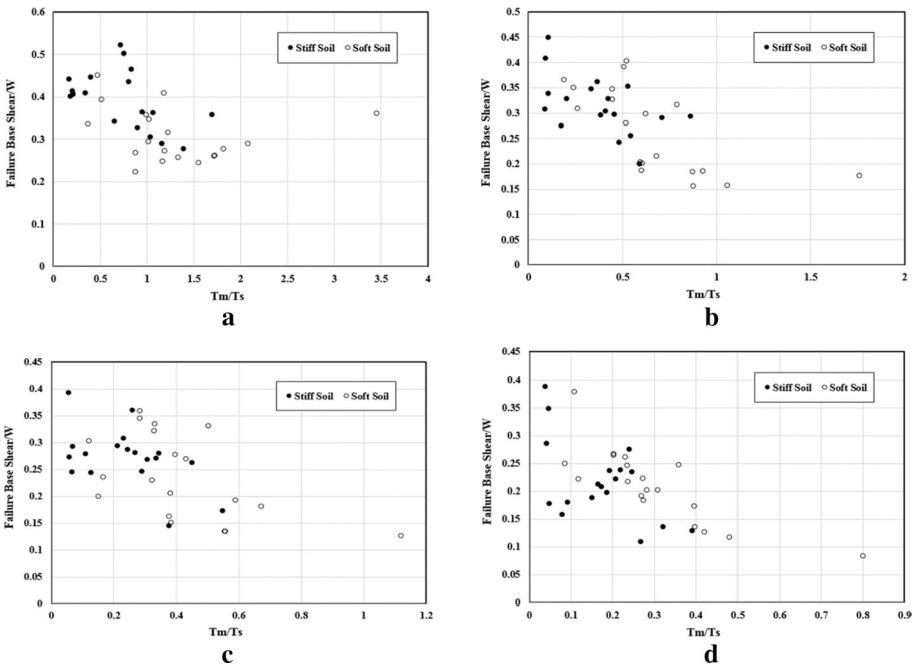

Fig. 13 The variation of the failure base shear with period ratio (T_m/T_s) for towers with a height of **a** 20 m, **b** 30 m, **c** 40 m and **d** 50 m

It should be noted that the failure base shear is normalized to the weight of the towers in the diagrams. Accordingly, the normalized base shear of the towers fall in the range of 0.1 to 0.55. Compared to the curves related to the effects of period ratio on failure PGA presented in the previous section, these diagrams exhibit higher dispersion. However, the failure base shear decreases with the increase in period ratio (T_m/T_s). In other words, the towers fail under a smaller lateral force when the period ratio, T_m/T_s, becomes larger. This

result is consistent with that obtained in the previous section regarding the effects of period ratio on the failure PGA.

5.3 The failure of towers

In the linear and nonlinear static analysis methods, the critical section of towers subjected to lateral loads is their base section where the maximum internal bending moment occurs. Therefore, it is expected that under earthquake ground shaking, damage to be concentrated at the bottom of the towers. The time history analyses conducted in this paper and the evaluation of tensile and compressive strains in different sections of towers under different ground motions indicate that the overturning mode of failure with development of cracks at the bottom of the towers is not always the dominant mode of failure in these slender structures. Comparing the failure of a specific tower under different earthquakes confirms that the ground motion not only influences the failure PGA, but also affects the failure location in height of the towers. It is noted that, usually when the period ratio, T_m/T_s, becomes smaller, flexural failure occurs at the upper sections of the tower causing instability and collapse of that section; an occurrence supported by actual observations from the past earthquakes [31]. In these cases, the failure PGA increases significantly. This behavior is clearer in the response of towers under the ground motions corresponding to the stations on soft soil. To better show this phenomenon, the average T_m/T_s that causes damage in the lower and upper half of the towers are plotted in Fig. 14. Accordingly, the average T_m/T_s that causes failure in the lower half of the towers is around 1.5 to 3.6 times that results in damage in the upper half, and this ratio decreases with increasing the height of the towers. Moreover, the mean T_m/T_s that causes failure in the upper half of the towers ranges 0.22 to 0.35 for towers with different heights.

6 Conclusions

In this study, the influence of frequency content of earthquake ground motion on the vulnerability of masonry towers was investigated. For this purpose, Incremental Dynamic Analysis was performed on four towers having different aspect ratios, using 37 ground motion records

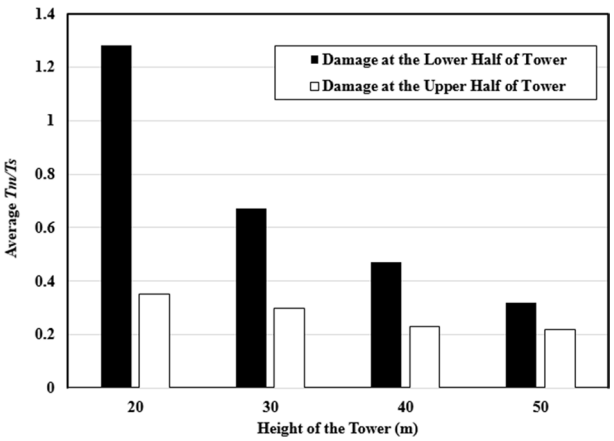

Fig. 14 The average T_m/T_s that causes damage in the lower and upper half of the towers

from sites with different types of soil. The towers were simulated by means of a validated idealized model. Furthermore, the mean period of the ground motion was utilized as the frequency content indicator. The major findings of this research are as follows:

1. The Equivalent Beam Element with fiber section is an efficient model requiring a relatively low computational effort for the nonlinear time history analysis of slender towers. The reasonably accurate free vibration and nonlinear analyzes of the Qutb Minar, as a relatively complicated structure using this model, confirms its acceptable performance.
2. The results of the Incremental Dynamic Analyses of towers confirm that in addition to the intensity of the ground shaking, other parameters such as frequency content of ground motion can affect the level of vulnerability of masonry towers. This result explains the survival of some historical masonry towers in past destructive earthquakes.
3. The period ratio, T_m/T_s, has a significant influence on the dynamic response of towers in terms of the failure PGA and base shear, as well as the failure mode of the structure. It was shown that, the failure PGA of the ground motion increases drastically when the period ratio is small (less than 0.1). The results also showed that the influence of period ratios greater than 0.5 on the failure PGA is negligible. It should be noted that this limit differs slightly for towers with different aspect ratios and vibration periods.
4. As the period ratio, T_m/T_s, becomes smaller, the shear force induced in the tower increases. This result is consistent with that presented regarding the failure PGA.
5. The level of stress and strains developed in the towers confirms that the frequency content of the ground motion has also a significant influence on the failure mode of the towers. When the period ratio becomes smaller, flexural cracks develop in the upper parts of the towers; leading to partial collapse of the tower.

7 Availability of data and material

Not applicable.

Appendix

See Tables 7, 8, 9 and 10.

Table 7 The characteristics of the ground motion records corresponding to the rock soil

Number	Event	RSN[a]	Moment magnitude, M_w	Site to source distance (km)	Event year
1	Chi-Chi, Taiwan	1245	7.62	36.06	1999
2	Chuetsooki, Japan	5006	6.80	77.65	2007
3	Duzce, Turkey	1613	7.14	25.78	1999
4	Hector Mine, US	3799	7.13	185.92	1999
5	Loma Prieta, US	804	6.93	63.03	1989
6	Niigata, Japan	4167	6.63	52.15	2004
7	Northridge-01, US	1091	6.69	23.10	1994
8	Sierra Madre, US	1649	5.61	37.63	1991
9	San Simeon, US	8167	6.52	37.92	2003
10	Whittier Narrows-01, US	680	5.99	6.78	1987
11	Anza-02, US	1943	4.92	28.79	2001
12	Chi-Chi-03, Taiwan	2687	6.20	93.15	1999
13	Chi-Chi-05, Taiwan	2996	6.20	49.84	1999
14	Tottori, Japan	3895	6.61	99.64	2000
15	Iwate, Japan	5483	6.90	37.45	2008
16	El Mayor-Cucapah, Mexico	5965	7.20	112.83	2010
17	Parkfield-02, US	8168	6.00	78.14	2004
18	San Fernando, US	59	6.61	89.37	1971

[a]Record Sequence Number

Table 8 The characteristics of the ground motion records corresponding to the soft soil

Number	Event	RSN	Moment magnitude, M_w	Site to source distance (km)	Event year
1	Chi-Chi, Taiwan	1209	7.62	24.13	1999
2	El Mayor-Cucapah, Mexico	5989	7.20	40.96	2010
3	Iwate, Japan	5471	6.90	46.77	2008
4	Coalinga-01, US	326	6.36	43.83	1983
5	Kocaeli, Turkey	1147	7.51	68.09	1999
6	Loma Prieta, US	759	6.93	43.77	1989
7	Northridge-01, US	962	6.69	45.44	1994
8	Superstition Hills-02, US	729	6.54	23.85	1987
9	Whittier Narrows-01, US	608	5.99	26.30	1987
10	Chi-Chi, Taiwan-05	2955	6.20	71.26	1999
11	Morgan Hill, US	452	6.19	53.89	1984
12	Yountville, US	1843	5.00	94.18	2000
13	Chi-Chi, Taiwan-02	2175	5.90	67.81	1999
14	Chi-Chi, Taiwan-03	2492	6.20	59.42	1999
15	Chi-Chi, Taiwan-04	2737	6.20	84.01	1999
16	Chi-Chi, Taiwan-06	3285	6.30	76.99	1999
17	Tottori, Japan	3962	6.61	45.98	2000
18	Niigata, Japan	4151	6.63	101.78	2004
19	Chuetsu-oki, Japan	4989	6.80	118.79	2007

Table 9 The mean period of the ground motions related to the rock soil

Record	RSN	Mean period (T_m) (s)
Chi-Chi, Taiwan	1245	0.50
Chuetsooki, Japan	5006	0.12
Duzce, Turkey	1613	0.42
Hector Mine, US	3799	0.53
Loma Prieta, US	804	0.60
Niigata, Japan	4167	0.10
Northridge-01, US	1091	0.40
Sierra Madre, US	1649	0.22
San Simeon, US	8167	0.95
Whittier Narrows-01, US	680	0.45
Anza-02, US	1943	0.10
Chi-Chi-03, Taiwan	2687	0.37
Chi-Chi-05, Taiwan	2996	0.65
Tottori, Japan	3895	0.12
Iwate, Japan	5483	0.19
El Mayor-Cucapah, Mexico	5965	0.78
Parkfield-02, US	8168	0.58
San Fernando, US	59	0.47

Table 10 The mean period of the ground motions related to the soft soil

Record	RSN	Mean period (T_m) (s)
Chi-Chi, Taiwan	1209	0.67
El Mayor-Cucapah, Mexico	5989	0.65
Iwate, Japan	5471	0.57
Coalinga-01, US	326	0.66
Kocaeli, Turkey	1147	0.87
Loma Prieta, US	759	0.75
Northridge-01, US	962	0.49
Superstition Hills-02, US	729	0.96
Whittier Narrows-01, US	608	0.49
Chi-Chi, Taiwan-05	2955	0.26
Morgan Hill, US	452	0.57
Yountville, US	1843	0.56
Chi-Chi, Taiwan-02	2175	0.29
Chi-Chi, Taiwan-03	2492	1.94
Chi-Chi, Taiwan-04	2737	0.69
Chi-Chi, Taiwan-06	3285	1.17
Tottori, Japan	3962	0.21
Niigata, Japan	4151	1.02
Chuetsu-oki, Japan	4989	0.96

Authors' contributions M.A. Najafgholipour: Conceptualization, Methodology, Validation, Investigation, Visualization, Writing original draft. H. Darvishi: Validation, Investigation, Writing—original draft. M.R. Maheri: Conceptualization, Writing—review and editing.

Declarations

Conflict of interest The authors declare that they have no competing interests.

References

Anzani A, Binda L, Carpinteri A, Invernizzi S, Lacidogna G (2010) A multilevel approach for the damage assessment of historic masonry towers. J Cult Herit. 11(4):459–470. https://doi.org/10.1016/j.culher.2009.11.008

ASCE/SEI 7-16 (2016) Minimum design loads and associated criteria for buildings and other structures. American Society of Civil Engineers, Reston

Bartoli G, Betti M, Marra AM, Monchetti S (2017a) Semiempirical formulations for estimating the main frequency of slender masonry towers. J Perform Constr Facil 31(4):04017025. https://doi.org/10.1061/(ASCE)CF.1943-5509.0001017

Bartoli G, Betti M, Monchetti S (2017b) Seismic risk assessment of historic masonry towers: comparison of four case studies. J Perform Constr Facil 31(5):04017039. https://doi.org/10.1061/(ASCE)CF.1943-5509.0001039

Bocciarelli M, Barbieri G (2017) A numerical procedure for the pushover analysis of masonry towers. Soil Dyn Earthq Eng 1(93):162–171. https://doi.org/10.1016/j.soildyn.2016.07.022

Casolo S, Milani G, Uva G, Alessandri C (2013) Comparative seismic vulnerability analysis on ten masonry towers in the coastal Po Valley in Italy. Eng Struct 1(49):465–490. https://doi.org/10.1016/j.engstruct.2012.11.033

Casolo S, Diana V, Uva G (2017) Influence of soil deformability on the seismic response of a masonry tower. Bull Earthq Eng. 15(5):1991–2014

Castellazzi G, D'Altri AM, de Miranda S, Chiozzi A, Tralli A (2018) Numerical insights on the seismic behavior of a non-isolated historical masonry tower. Bull Earthq Eng 16(2):933–961. https://doi.org/10.1007/s10518-017-0231-6

Cavalagli N, Comanducci G, Gentile C, Guidobaldi M, Saisi A, Ubertini F (2017) Detecting earthquake-induced damage in historic masonry towers using continuously monitored dynamic response-only data. Procedia Eng 1(199):3416–3421. https://doi.org/10.1016/j.proeng.2017.09.581

Iranian National Building Code (part 6): loading (2013)

D'Ambrisi A, Mariani V, Mezzi M (2012) Seismic assessment of a historical masonry tower with nonlinear static and dynamic analyses tuned on ambient vibration tests. Eng Struct 1(36):210–219. https://doi.org/10.1016/j.engstruct.2011.12.009

de Silva F, Pitilakis D, Ceroni F, Sica S, Silvestri F (2018) Experimental and numerical dynamic identification of a historic masonry bell tower accounting for different types of interaction. Soil Dyn Earthq Eng 1(109):235–250. https://doi.org/10.1016/j.soildyn.2018.03.012

Diaferio M, Foti D, Potenza F (2018) Prediction of the fundamental frequencies and modal shapes of historic masonry towers by empirical equations based on experimental data. Eng Struct 1(156):433–442. https://doi.org/10.1016/j.engstruct.2017.11.061

Facchini L, Betti M, Corazzi R, Kovacevic VC (2017) Nonlinear seismic behavior of historical masonry towers by means of different numerical models. Procedia Eng 1(199):601–606. https://doi.org/10.1016/j.proeng.2017.09.103

FEMA F (2000) Recommended seismic design criteria for new steel moment-frame buildings. FEMA-350

García-Macías E, Ubertini F (2019) Seismic interferometry for earthquake-induced damage identification in historic masonry towers. Mech Syst Signal Process 1(132):380–404. https://doi.org/10.1016/j.ymssp.2019.06.037

Hickey J, Broderick B (2019) Influence of mean period of ground motion on inelastic drift demands in cbfs designed to eurocode 8. Eng Struct 1(182):172–184. https://doi.org/10.1016/j.engstruct.2018.12.055

Invernizzi S, Lacidogna G, Lozano-Ramírez NE, Carpinteri A (2019) Structural monitoring and assessment of an ancient masonry tower. Eng Fract Mech 1(210):429–443. https://doi.org/10.1016/j.engfracmech.2018.05.011

Kumar M, Castro JM, Stafford PJ, Elghazouli AY (2011) Influence of the mean period of ground motion on the inelastic dynamic response of single and multi degree of freedom systems. Earthq Eng Struct Dyn 40(3):237–256. https://doi.org/10.1002/eqe.1013

Lee J (2009) Engineering characterization of earthquake ground motions. PhD diss

Maheri MR (2004) Seismic vulnerability of post-Islamic monumental structures in Iran: review of historical sources. J Archit Eng 10(4):160–166. https://doi.org/10.1061/(ASCE)1076-0431(2004)10:4(160)

Maheri MR, Khajeheian MK, Vatanpour F (2019) In-plane seismic retrofitting of hollow concrete block masonry walls with RC layers. Structures 20:425–436. https://doi.org/10.1016/j.istruc.2019.05.008

Marra AM, Salvatori L, Spinelli P, Bartoli G (2017) Incremental dynamic and nonlinear static analyses for seismic assessment of medieval masonry towers. J Perform Constr Facil 31(4):04017032. https://doi.org/10.1061/(ASCE)CF.1943-5509.0001022

Mendes N (2006) Analise estrutural do minarete Qutub Minar. Universidade do Minho, Guimaraes (in Portuguese)

Micelli F, Cascardi A (2020) Structural assessment and seismic analysis of a 14th century masonry tower. Eng Fail Anal 1(107):104198. https://doi.org/10.1016/j.engfailanal.2019.104198

Najafgholipour MA, Maheri MR, Lourenco PB (2014) Definition of interaction curves for the in-plane and out-of-plane capacity in brick masonry walls. Constr Build Mater 55C:168–182. https://doi.org/10.1016/j.conbuildmat.2014.01.028

Najafgholipour MA, Maheri MR, Darvishi H, Dehghan SM (2019) A semi-analytical formulation for estimating the fundamental vibration frequency of historical masonry towers. Bull Earthq Eng 17(5):2627–2645. https://doi.org/10.1007/s10518-018-00552-6

Peña F, Lourenço PB, Mendes N, Oliveira DV (2010) Numerical models for the seismic assessment of an old masonry tower. Eng Struct 32(5):1466–1478. https://doi.org/10.1016/j.engstruct.2010.01.027

Pintucchi B, Zani N (2014) Effectiveness of nonlinear static procedures for slender masonry towers. Bull Earthq Eng 12(6):2531–2556. https://doi.org/10.1007/s10518-014-9595-z

Preciado A (2015) Seismic vulnerability and failure modes simulation of ancient masonry towers by validated virtual finite element models. Eng Fail Anal 1(57):72–87. https://doi.org/10.1016/j.engfailanal.2015.07.030

Rathje EM, Faraj F, Russell S, Bray JD (2004) Empirical relationships for frequency content parameters of earthquake ground motions. Earthq Spectra 20(1):119–144. https://doi.org/10.1193/1.1643356

Romaro F (2011) A study on seismic behaviour of masonry towers. Doctoral dissertation, University of Trento

Saisi A, Gentile C, Guidobaldi M, Xu M (2015) Dynamic monitoring and seismic response of a historic masonry tower. In: Key engineering materials, vol 628. Trans Tech Publications Ltd, pp 55–60. https://doi.org/10.4028/www.scientific.net/KEM.628.55

Sarhosis V, Milani G, Formisano A, Fabbrocino F (2018) Evaluation of different approaches for the estimation of the seismic vulnerability of masonry towers. Bull Earthq Eng. 16(3):1511–1545. https://doi.org/10.1007/s10518-017-0258-8

Shakya M, Varum H, Vicente R, Costa A (2016) Empirical formulation for estimating the fundamental frequency of slender masonry structures. Int J Archit Herit 10(1):55–66. https://doi.org/10.1080/15583058.2014.951796

Silva FD (2020) Influence of soil-structure interaction on the site-specific seismic demand to masonry towers. Soil Dyn Earthq Eng. https://doi.org/10.1016/j.soildyn.2019.106023

Torelli G, D'Ayala D, Betti M, Bartoli G (2020) Analytical and numerical seismic assessment of heritage masonry towers. Bull Earthq Eng 18(3):969–1008. https://doi.org/10.1007/s10518-019-00732-y

Valente M, Milani G (2016a) Non-linear dynamic and static analyses on eight historical masonry towers in the North-East of Italy. Eng Struct 1(114):241–270. https://doi.org/10.1016/j.engstruct.2016.02.004

Valente M, Milani G (2016b) Seismic assessment of historical masonry towers by means of simplified approaches and standard FEM. Constr Build Mater 1(108):74–104. https://doi.org/10.1016/j.conbuildmat.2016.01.025

Vamvatsikos D, Cornell CA (2002) Incremental dynamic analysis. Earthq Eng Struct Dyn 31(3):491–514. https://doi.org/10.1002/eqe.141

Xie Q, Xu D, Zhang Y, Yu Y, Hao W (2020) Shaking table testing and numerical simulation of the seismic response of a typical China ancient masonry tower. Bull Earthq Eng 18(1):331–355. https://doi.org/10.1007/s10518-019-00731-z